Rapid Cutting and Drilling of Transparent Materials via Femtosecond Laser Filamentation

Simas BUTKUS[*1], Domas PAIPULAS[*1], Romualdas SIRUTKAITIS[*2], Eugenijus GAIŽAUSKAS[*1] and Valdas SIRUTKAITIS[*1]

[*1]*Vilnius University, Faculty of Physics , Department of Quantum Electronics, Laser Research Center, Saulėtekio av. 10, Vilnius 10223, Lithuania*
[*2]*Vilnius University, Institute of Biochemistry, Mokslininkų str.12, Vilnius 08622, Lithuania*
Simas.Butkus@ff.vu.lt

Microfabrication of transparent materials using femtosecond laser pulses has showed good potential towards industrial application. Maintaining pulse energies above the critical self-focusing limit produced filaments that were used for micromachining purposes. This article demonstrates two different fabrication techniques using femtosecond filaments generated in water which is in contact with the transparent sample. Both methods yielded through holes made in soda-lime and fused silica glass samples which had thickness up to 1 mm. These fabricated holes have an aspect ratio close to 20; moreover, the fabrication time is of the order of tens of seconds.
DOI:10.2961/jlmn.2014.03.0006

Keywords: femtosecond micromachining, ablation, filament, etching, fused silica

1. Introduction

Femtosecond laser systems are widely applied in various scientific and industrial fields (medicine, material research, metrology, telecommunication, energy research, etc) [1]. Due to the forever growing industrial demand for quality and fast fabrication of transparent materials, these laser systems are rapidly becoming a topic of interest in industry. Sapphire dicing, flat panel rapid cutting, hardened glass processing, light extractor fabrication for LED technologies, integration of microfluidic devices, diamond processing attain great attention from industry players. Microfabrication of transparent materials is becoming essential due to increasing industrial requirements of micrometer scale high-quality devices [2]. Though conventional methods (diamond drilling, water jet drilling, micro sand blasting) are still applicable [3], the production of cracks, low fabrication rates and aspect ratios, limitations towards 3D microfabrication may open new frontiers towards industrial applications of femtosecond laser microfabrication.

Femtosecond pulse microfabrication (high intensity- TW/cm^2) differs from low intensity (CW, nanosecond- kW/cm^2) fabrication systems. High intensity pulses result in nonlinear absorption of energy whereas low intensity pulses can be absorbed by the material only if the energy of the photon is no less than the band gap of the material. At high intensity limits, certain materials cease to be transparent due to strong nonlinear absorption, thus enabling fabrication of virtually any type of material regardless of the wavelengths the laser is emitting [4]. Moreover, typical femtosecond pulses are two orders shorter in duration than the electron-phonon relaxation time thus the laser affected zone is vaporized faster than the energy can be transferred to the surrounding regions, making precision fabrication possible. Though the femtosecond laser appears superior to other types of lasers in almost every aspect, currently, high average power and high repetition rate lasers are not very common. Therefore, optimization of the fabrication process is vital.

A great number of articles have been published on femtosecond laser microfabrication of transparent materials where the main material removal mechanism is direct laser ablation. Ablation mechanisms can be implemented for material processing using various fabrication strategies: front side and water-assisted back side ablation [5–9], ablation enhanced by spatial and temporal focusing [10–12]. In addition, alternative fabrication techniques are also present: chemical etching of laser induced bulk modifications [13–18], glass dicing techniques [19, 20]. Although the above mentioned techniques are capable of producing relatively high-quality holes, the need for high numerical aperture (NA) focusing, fast motion translation stages can severely prolong the fabrication process. These limitations primarily occur because fabrication is typically performed with parameters that are below critical self-focusing limits in order to avoid filamentation, which is an undesirable effect for the stated fabrication methods. Moreover, in the absence of optimal fabrication parameters, cracks and holes showing conicity are probable. [21]

In this work we present transparent material cutting and drilling results achieved with a fabrication setup that employs filamentation. By applying a water layer on top of the glass samples with the ability to change the thickness (from 0.6 to 1.7 mm when necessary) of the layer and using a low NA objective, filaments can be created at the surface of the glass. Filaments are formed within the water layer. At the core of the filament, strong electron plasma generation and electron relaxation causes *ablation* at the surface or *modifications* susceptible to certain etchants in the bulk [22] of the glass samples. In this

2D hole cutting and drilling technique filamentation is in fact fa-vorable because due to its surplus focusing abilities, complex z axis positioning systems and sharp focusing optics can be elim-inated. Moreover, it enables the use of galvanometric scanners in combination with f- theta lenses producing large scanning fields and scanning rates of the order of m/s or greater. The complexity of this system was brought to a minimum bearing in mind that non scientific personnel might be the end-user of such a system.

2. Experimental setup

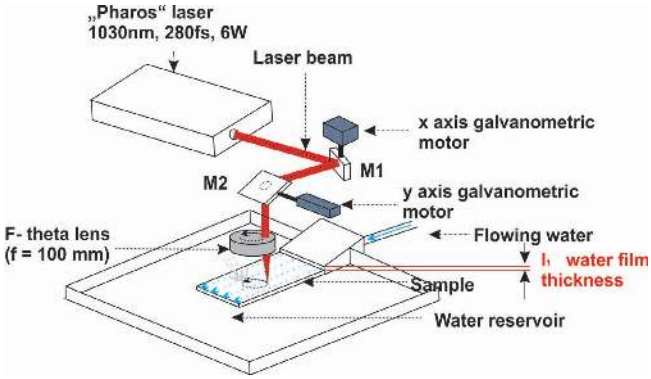

Fig. 1: The experimental setup of the microfabrication system.

The experiments were carried out using the Yb:KGW femtosecond laser system "Pharos" (Light Conversion Ltd). The two axis galvanometric scanners (ScanLab Inc.) were controlled by fabrication software SCA (Altechna Ltd). Fig. 1 shows a schematic drawing of the experimental setup. The laser beam was deflected by the scanners and focused with a 100 mm f-theta lens on the glass samples. Drilling and cutting was carried out in soda-lime glass (thickness - 1 mm), fused silica glass (FS) (thickness –2 mm) and ultraviolet fused silica glass (UVFS) (thicknesses –3 mm and 0.5 mm) samples. The samples were covered with a thin water film created by injecting water through a nozzle. The thickness of this film (l_1) was varied by controlling the speed of the water flow along the surface of the sample through variation of pressure inside the nozzle. Due to surface tension effects the water film is thicker at lower water flow rates, and thinner at higher flow rates. The thickness of this film was measured by shining a beam from a green laser pointer onto the surface of the water film at an angle of about 45 degrees and measuring how the position of the reflected beam (from the water layer) changes on a CCD camera. It was found that the thickness of the film can be determined to an accuracy better than 10 μm. Typical writing parameters were chosen as follows: average pulse power – 4.7 W, pulse duration – 280 fs, repetition rate – 25 kHz – 100 kHz, wavelength – 1030 nm, focal spot diameter– 55 μm.

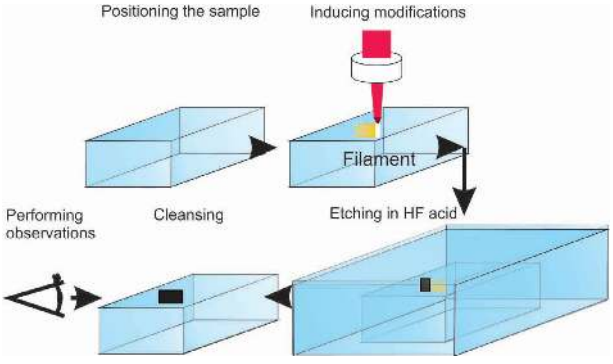

Fig. 2: Simplified schematic drawing of the fabrication process when material modifications, created in the bulk of the glass with femtosecond filament, are later etched in HF acid.

Two types of experiments were conducted: (1) material modification via filamentation in the glass sample (without the additional water layer ($l_1 = 0$)) and subsequent chemical etching, and (2) filament formation in the water film and material removal via glass surface ablation. By varying the thickness of the water, different results were obtained. For comparison, an experiment of glass ablation without the water layer was also carried out.

3. Results and discussion

3.1. Filament induced modification formations and etching

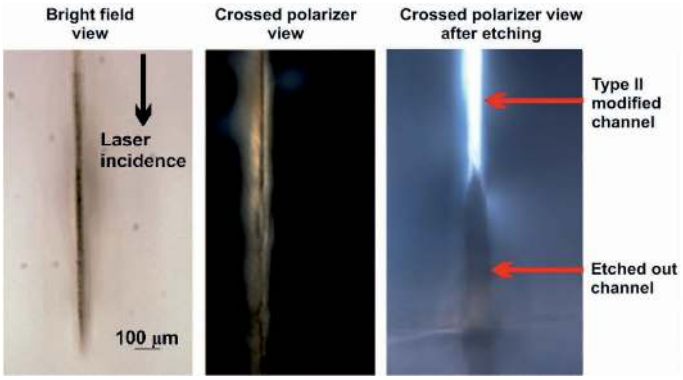

Fig. 3: Typical modified birefringent regions (*left,middle*) and an etched-out region (*right*) in fused silica. These sort of modifications form after a hundred sample translations at a scanning speed equal to 10 mm/s, the lenght of these modified channels was set to 6 mm overall equaling to a fabrication time of 1 minute. The repetition rate was set to 100 kHz, other parameters were the same as stated in section 2.

It is well known that three types of modifications can be induced in fused silica with femtosecond laser pulses: homogeneous refractive index change (so called Type I modification), birefringent modifications (Type II) and voids or micro cracks (Type III) [23, 24]. It was shown that modification of Type II could be up to 300 times more prominent to chemical etching (in HF acid) than that of Type I, i.e. the modified regions dissolve in acid 300 times faster than unmodified regions [25]. The exact reasons for the formation of Type II modifications is still a debatable topic however studies have shown [25] that these modifications can be attributed to nano crack formations in the laser affected zones. These nano cracks help the etchant to penetrate into the glass and ultimately dissolve the laser affected zones faster. If insufficient energy is deposited (absorbed) in

the volume then the nanocracks will not form and the etchant will have a uniform effect throughout the sample. If too much energy is absorbed, voids (Type III modifications) develop and the required nano crack formation will be disrupted. Therefore a range of pulse energies are present (given specific focusing conditions) that are usable for Type II modification formation. This technique can be used for hollow 3D channel or pattern integration in selected transparent materials [26] and widely applicable for microfluidic sensor fabrication [13]. Such behavior can be also utilized for rapid drilling with filaments. A simplified schematic drawing of the steps required for this process is given in Fig. 2.

Type II modifications are observable (in our experimental setup) at a wide range of laser parameter values. The modifications presented here were formed using a laser repetition rate of 100 kHz, and an average laser power equaling 4.7 W. The focal position was set to be approximately 2 mm beneath the surface of the sample. By varying focal position (actual position of the laser focus relative to the surface of the sample), pulse energy or repetition rate, filament formation and hence, birefringent modifications (Type II) are induced at different positions relative to the surface of the sample. In this way, modified regions ranging from several hundred micrometers to several millimeters in length could be achieved. Thus, modified regions can be extended when filamentation is employed. Changes in focal position alter the fluence at the surface of the sample, therefore self-focusing is either more or less pronounced. However, electron plasma generation at higher depths is weaker, due to the longer length that the laser pulse has to travel prior to filamentation, thus the homogeneity of a long channel is compromised. Long modified regions can also be achieved by varying the repetition rate of the laser, but keeping the average laser power (such features are present in such laser systems as Pharos) and focal position constant. Change in repetition rate gives change to the energy of the pulse, which varies the position of the filament due to more or less pronounced self-focusing. By scanning the beam with different laser repetition rates, long channels can be formed without the need of focal position change (in our case, the optimal focal position was 2 mm below the sample's surface). These results are obtained again due to the different fluence values hitting the surface of the sample.

When observing modified fused silica samples using a cross-polarized optical microscope mode, by presence of induced optical birefringence we can identify that these modifications are Type II modifications (Fig. 3). In contrast, soda-lime glass samples did not posses such modifications and only color center formation were apparent. Volumetric Type II modifications are observable only in some materials (fused silica, sapphire) while other glasses do not posses this property. This shows that nano crack formations are also influenced by the chemical composition of the material [27].

After inducing modifications in both types of glasses, the samples were submerged in a 5% (volume percentage) HF acid solution for 6 hours. Fused silica samples showed several hundred micrometers deep etched-out channels, whereas soda-lime glass tends to dissolve evenly through out the whole sample. Fig. 3 (right) illustrates an etched-out channel in fused silica glass after 6 hours of etching. It is important to note, that this channel was etched-out from the sample's back surface. Despite what focal position or pulse energy was chosen, modified regions that start from the front surface were not achieved. Modified channels that are in contact with the surface (front or back) are essential for the application of this method in order for the etchant to have any desirable effect, i.e. if the modified channel is formed only in the bulk (shielded by unmodified regions) then the etchant can not reach the laser processed regions and selective material removal can not be carried out and the whole sample dissolves evenly. It is worth pointing out that 6 hours of etching is a relatively long time and the entire process may appear as extremely slow, however if a great quantity of samples are prepared (modifications are formed within the samples) then they can be submerged simultaneously and the etching time will fade in comparison to the time required to make the modifications. Therefore if modified channels could be prepared quickly enough then the entire process can be time efficient when greater quantities of samples are prepared.

A dependency on the beam scanning speed was noticed. Type II modifications tended to form at relatively slow scanning rates. It is known that Type II modifications form most efficiently during multipulse exposure [28], therefore, slower scanning speeds result in increased pulse overlap. Thus in our experiments optimal scanning speed was in the range of 1 – 10 mm/s. A through hole with 2 mm diameter was *cut* in a 0.5 mm thick UVFS sample by this method in about one minute of laser fabrication (plus additional 6 hours of post processing etching in HF acid). A modified track (Type II) was formed in the bulk of the sample (modified regions are in contact only with the back surface) by continuously rotating the laser beam along the perimeter of the hole for 1 minute at a 10 mm/s linear scanning speed (repetition rate – 100 kHz, focused 2 mm below the surface). Afterwards, the focal position was shifted to the sample's front surface and ordinary ablation was carried out for 10 seconds with the same parameters in order to ablate 50 - 70 μm deep channels to reach the Type II modified z one. The sample then was chemically etched and the through hole was completed. The etching rate was calculated to be approximately 0.45 μm/min, which is roughly 200 times faster than the unmodified r egions. In addition, through variation of focal position relative to the surface of the sample a 4.6 mm long modified channel susceptible to chemical etching was fabricated. It is worth mentioning that variation in other parameters that were kept constant (see section 2) would yield different results. Shorter wavelengths would results in lower order nonlinear absorption and a decrease in the critical power required for self-focusing, i.e. filamentation would be more easily achieved and possibly greater absorption of the energy would commence. This in turn would produce modifications slightly faster, however the process of at least second harmonic generation would produce high energy losses (depending on the crystals chosen but as high as 50 %) and would add to the

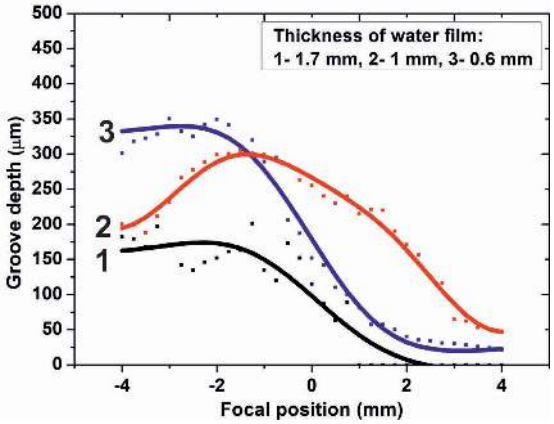

Fig. 4: Different groove depths achieved in soda-lime glass at different focal position values and thicknesses of the water layer. The focal position is measured from the sample's surface and negative values mean – below the surface. The solid lines are guides for the eye.

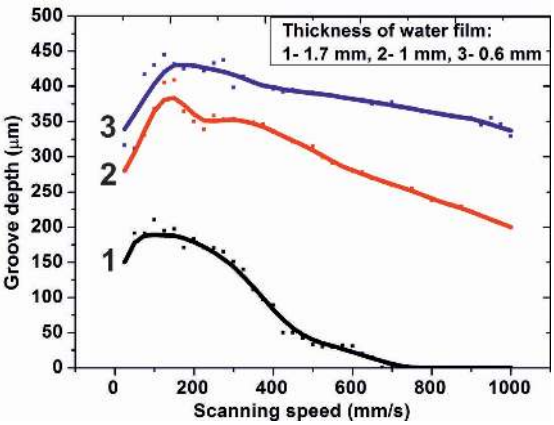

Fig. 5: Different groove depths achieved in soda lime glass at different beam scanning speeds and thicknesses of the water layer. The focal position was set 2 mm below the surface of the sample. The solid lines are guides for the eye.

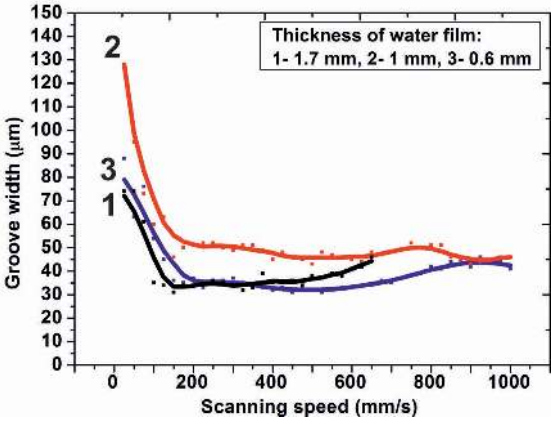

Fig. 6: Different groove widths achieved at different beam scanning speeds and thicknesses of the water layer. The solid lines are guides for the eye.

complexity of the system therefore the slight increase in effi-ciency would not be enough to justify the effort. Change in pulse duration and focusing conditions would greatly change the intensity of the arriving pulse. This would also add to more or less pronounced self-focusing. Since lower intensity pulses would result in a lower free electron density in the core of the filament, increase in pulse duration and decrease in the focal spot diameter would decrease the efficiency of the entire pro-cess, in addition, sharper focusing conditions would result in greater sensitivity of the system.

3.2. Cutting and drilling of transparent materials with fem-tosecond filament formed in thin water layer

A different strategy for transparent material drilling is to use direct ablation from the top sample's surface, while the ablation in this case is induced by the laser filament. In this configuration, chemical post-processing is not necessary (holes are drilled on the spot) and the range of the materials that can be processed widely increases because this process only mildly depends on the chemical composition of the material. As was mentioned earlier, the water layer on the top of the sample acts as a buffer layer where filamentation appears. Its thickness can be controlled by utilizing a variable water flow rate along the sample's surface. In addition, this layer helps reduce thermal effects and remove debris from the processed surface. It is worth pointing out that the water film can additionally increase the ablation rate through a process known as laser-induced plasma confinement. The plasma that is being formed at the glass sample's front surface is being confined via the water layer, which results in better plasma-target coupling [29, 30] and the interaction of the plasma with the glass is being pro-longed which results in more efficient ablation. By varying the focal position and beam scanning rate it is possible to change filament position in respect to the sample surface. Therefore the key for efficient fabrication is to find the right laser parameters that not only produce strong absorption in the sample (efficient ablation), but also induce water boiling and evaporation that enhances debris removal from the ablated channel. In addition, water reduces thermal stress through cooling. Therefore, the balance between energy losses in water and in glass is crucial for efficient fabrication.

The thickness of the water layer on top of the sample has significant impact on groove quality and depth. An investigation on how the thickness of the water influences the depth of the grooves was carried out. By varying the thickness of the water film and keeping the number of sample translations constant (number of repetitions at fixed scanning rate) grooves having different depths were produced. These results are presented in Fig. 4. All grooves were made with parameters depicted in section 2 (rep. rate – 25 kHz), while the scanning speed was set to 400 mm/s. Each fabricated groove was 6 mm in length and the fabrication time of each groove was 10 s. When fabricating at relatively high water film thickness values ($\geq$ 1.7mm), the maximum groove depth equaled approximately 100 μm. Using thinner water layers better results were obtained. Fig. 4 shows that the maximum groove depth was achieved at the thinnest

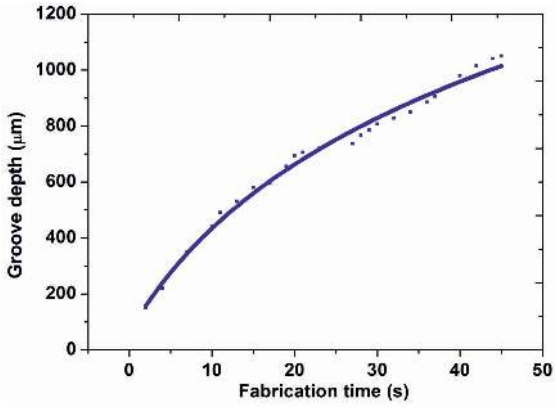

Fig. 7: Groove depth versus fabrication time while cutting soda-lime glass using optimal parameters (see text). The length of the groove equals 6 mm.

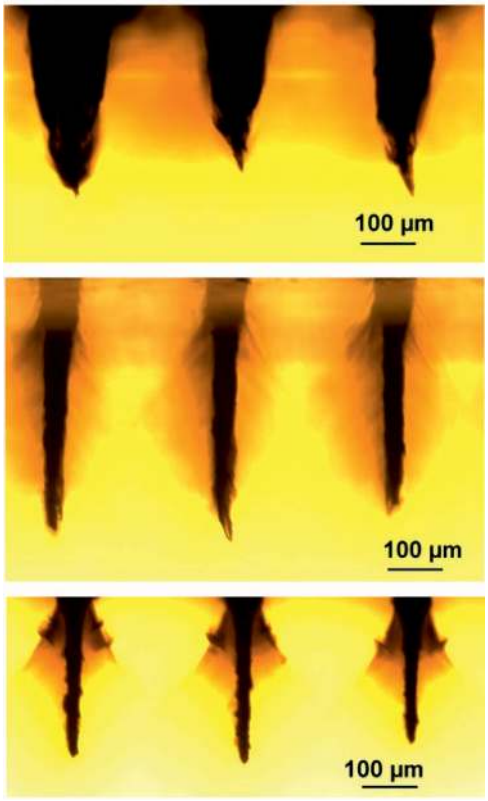

Fig. 8: Typical groove profiles made in soda-lime glass at different scanning speeds: 50 mm/s (top), 150 mm/s (middle), 500 mm/s(bottom). Water layer thickness was equal to 0.6 mm.

water layer values (in our experimental setup, the thinnest layer was equal to 0.6 mm).

These results could be explained by taking into account the nonlinearities of the medium (water) that are invoked due to the extreme intensities of these pulses (the critical power for self focusing is exceeded roughly by 100 fold in these experimental conditions). Given these conditions due to self-focusing, multiphoton absorption and diffraction filamentary propagation occurs after a certain distance from the front surface of the

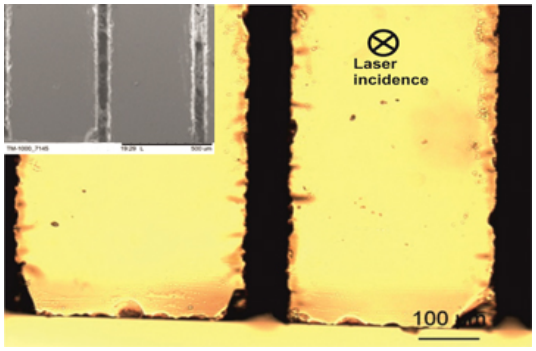

Fig. 9: Optical image of top surface of the fabricated grooves using optimal fabrication parameters. Inset shows a SEM image of the same area.

water film. These effects are cumulative and require specific propagation in the medium to manifest [31]. It was recently showed through theoretical modeling that an intense filament will appear after 0.5 mm of propagation in water given similar experimental conditions and the highest intensity values are reached at the starting point of the filament [32]. Therefore an increase in the thickness of the water film results in higher pulse energy depletion in the water: a thicker water film results in decreased ablation efficiency whereas a thinner film gives better ablation efficiency results. However if the film thickness is less than approximately 0.5 mm it is thought that the ablation efficiency will start decreasing again due to insufficient propa-gation distance required for filamentation. In our experimental setup, the minimal film thickness that was achievable was 0.6 mm, thus the expected decrease in ablation efficiency when the thickness is lower than 0.6 mm could not be experimentaly verified.

The existence of the optimal focal position beneath the surface of the sample can be explained in a similar way: as stated electron generation is strongest at the starting point of the filament, therefore if the filament forms far above the surface of the sample higher nonlinear losses are present in the water. The optimal focal position – 2 mm beneath the surface of the sample means that the filament appears right on top of the surface of the sample in the water layer.

A series of experiments were conducted in order to determine a dependency of scanning speed on resulted groove depths. These results are depicted in Fig. 5 (the focal position was chosen as the optimal from the previous experiment). As in the previous example, 6 mm length grooves were fabricated in

soda-lime glass, where each groove was processed for 10 s at different beam scanning speeds (thus the total exposure per groove was constant). Again, a strong dependency on deeper grooves is evident at thinner water film thickness values. The deepest grooves were achieved at the minimal water film thickness value though an explanation for the maximum depth value centered around a particular scanning speed value might be more complicated. Bearing in mind that there exists a set of optimal conditions at which the efficiency of the fabrication process is highest, these conditions yield maximum nonlinear absorption occurring at the sample, efficient cleansing of the

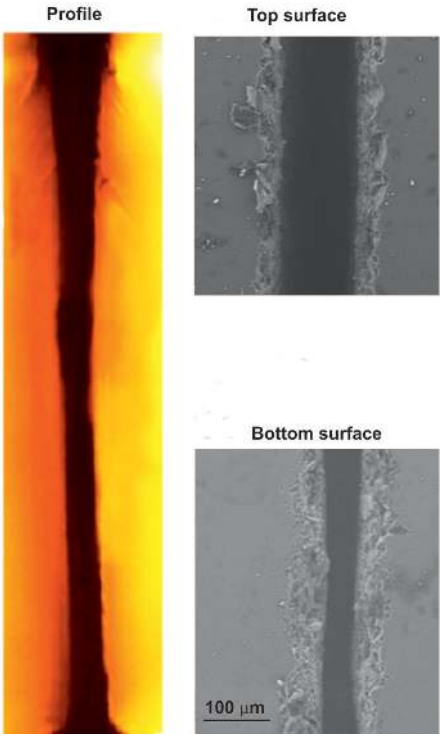

Fig. 10: Cross-section of a 1 mm deep channel drilled in soda-lime glass. The aspect ratio of this groove equals 20. Also SEM images of the top and bottom surfaces are shown.

groove due to cavitation bubble induced cleaning [33], plasma confinement, effective cooling of the sample that prevents fracturing and etc. All these conditions arise due to different pulse overlap values. At a scanning speed equal to 125 mm/s and a repetition rate – 25 kHz, 11 laser pulses overlap in series, whereas at a scanning speed equal to 675 mm/s, only 3 pulses overlap in series. After a series of overlapping pulses the water region can be transformed into a mixture of water and vapor or vapor. This would explain the increased groove widths at low scanning speeds depicted in Fig. 6. At lower scanning speeds due to the strong pulse overlap, the water is being evaporated faster from the surface of the sample than it can be replenished. If this occurs, the material is being removed via ablation without water, thus giving wide and shallow groove profiles. The actual groove profiles fabricated at different scanning speeds differ widely. An illustration of groove profiles is shown in Fig. 8. Grooves fabricated at a scanning speed equal to 50 mm/s showed relatively wide and shallow profiles, whereas grooves fabricated at 500 mm/s are substantially narrower, however, prone to cracking at the surface. Grooves fabricated at 150 mm/s were not as prone to cracking as grooves fabricated at higher scanning speeds, moreover, these grooves appear deeper with steep edges. The deepest grooves were formed using these fabrication parameters: focal position- 2 mm beneath the front surface of the sample, water film thickness- 0.7 mm, scanning speed- 125 mm/s. A typical surface view of a the fabricated channel is shown in Fig. 9.

A dependency of groove depth versus fabrication time in 1 mm thick soda-lime glass was studied using the optimal parameters and is shown in Fig. 7. This dependence takes the form of a logarithmic function and is a result of decreased cleansing efficiency due to increased depth and decreased fluence due to higher nonlinear absorption of the laser pulse in the water caused by a longer propagation length. Though scanning electron microscope (SEM) images showed a surface free of cracks observations with an optical microscope revealed that crack formations are present in the bulk. The exact reasons why these cracks form in the bulk are not entirely understood. After drilling through holes (Fig. 10), it can be noted that the width of the grooves stays constant at approximately 40-50 μm. A 1 mm deep, 6 mm long channel was drilled in soda-lime glass, the fabrication of this channel took approximately 40 seconds. This demonstrates that relatively quick glass cutting can be achieved with this technique, moreover, glass cutting can be implemented in any desired shape. As a demonstration a complex form object – 36 angle sprocket, cut in a 1 mm thick soda lime glass sample is shown in Fig. 11. All cutting procedure took less than 4 minutes.

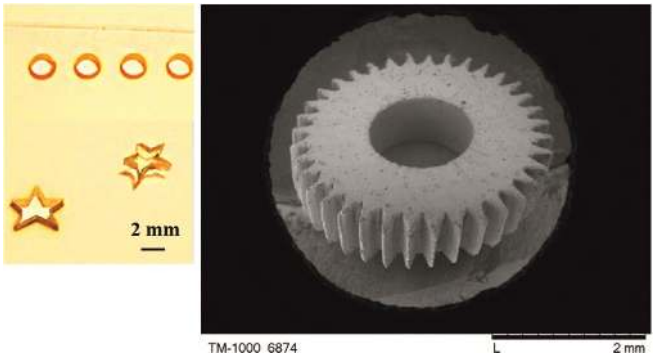

Fig. 11: Complex shape objects fabricated in 1 mm thick soda-lime glass.

Furthermore, for comparative reasons a glass cutting experiment was conducted without the additional water layer. Here, the material removal mechanism is direct ablation by a Gaussian beam. The optimal focal position was found to be precisely on the surface of the sample. A deepest groove reaching approximately 200 μm was formed after 10 seconds of laser fabrication time, however, further fabrication caused complete shattering of the sample (Fig. 12 (right)). Thus, strong crack formations

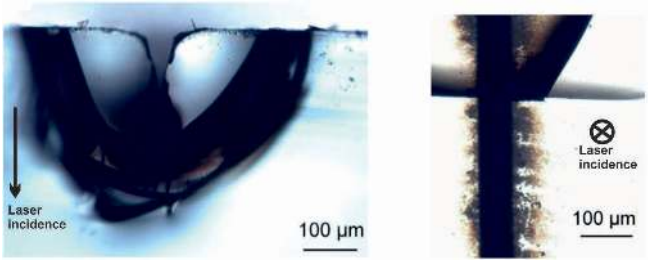

Fig. 12: Strong crack formations (black areas) after laser fabrication in soda-lime glass without water. Left– groove profile, right–groove top view. The horizontal dark line (right picture) is a crack that formed throughout the whole sample severing it in two pieces due to thermal stress.

prevent through hole fabrication. The black areas around the laser impingement zone are crack formations caused by thermal stress. Due to this thermal stress the sample can shatter entirely throughout its whole volume. A dependency on scanning speed was not evident in these experiments. These results clearly show that the additional water layer on top of the samples sufficiently improves cutting efficiency and quality.

4. Conclusion

A fabrication system has been built for rapid cutting of holes and other complex-shaped objects in fused silica and soda-lime glasses with high intensity femtosecond pulse generated filaments. We have showed that the intensity at the core of the filament is sufficient to induce structural changes within the bulk of transparent materials and cutting can be achieved in fused silica by inducing modified regions that are susceptible to chemical etching. In addition direct ablation of glass samples with laser filaments can be realized by introducing a thin water layer above the sample. We showed that such a water layer suf-ficiently improves the quality of the cuts, also it decreases the processing time. We demonstrated that with such a technique it is possible to drill holes with 2 mm diameter in 1 mm thick soda-lime glass in less than 40 s. The fabrication of complex shape objects is also demonstrated.

Acknowledgments

The authors thank the European Social Fund Agency for the support according to research grant No. VP1-3.1-SMM-10-V-02-007 (Development and utilization of new generation industrial laser material processing using ultrashort pulse lasers for industrial applications).

References

[1] W. Sibbett, A. A. Lagatsky and C. T. A. Brown: Opt. Expr., 20(7), (2012) 6989.

[2] R. Buividas, M. Mikutis, T. Kudrius, A. Greiˇcius, G. Šlekys and S. Juodkazis: Lith. Journ. of Phys., 52(4), (2012) 301.

[3] D.J. Hwang, T.Y. Choi and C.P. Grigoropoulos: J. Appl. Phys., 79, (2004) 605.

[4] Ch. B. Schaffer, A. Brodeur and E. Mazur: Meas. Sci. Technol., 12, (2001) 1784.

[5] A. Ran, L. Yan, D. Yan-Ping, F. Ying, Y. Hong and G. Qi-Huang: Chinese Phys. Lett., 21, (2004) 2465.

[6] Z. Wu, H. Jiang, Q. Sun, H. Guo, H. Yang and Q. Gong:Appl. Opt., 6, (2004) 671.

[7] R.L. Byer, A. Harkin, J. Ashmore, H.W. Stone, M. Shen and E. Mazur: Appl. Phys. Lett., 83, (2003) 3030.

[8] Ch. B. Schaffer, A. Brodeur, J. F. Garcia, and E. Mazur: Opt. Lett., 26, (2001) 2.

[9] D. Ye, Y. Guang-Jun, W. Guo-Rui, M. Hong-Liang, Y. Xiao-Na, and M. Hong: Chin. Phys. B., 21, (2012) 201.

[10] D. N. Vitek, D. E. Adams, A. Johnson, Ph. S. Tsai, S. Backus, Ch. G. Durfee, D. Kleinfeld, and J. A. Squier: Opt. Expr.,18(17), (2010) 18086.

[11] D. N. Vitek, E. Block, Y. Bellouard, D. E. Adams, S. Backus, D. Kleinfeld, Ch. G. Durfee and J. A. Squier: Opt. Expr., 18(24), (2010) 24673.

[12] E.Block, M. Greco, D. Vitek, O. Masihzadeh, D. A. Ammar, M. Y. Kahook, N. Mandava, Ch. Durfee and J. Squier: Opt. Expr., 4(6), (2013) 831.

[13] Y. Bellouard, A. Said, M. Dugan and Ph. Bado:Opt. Exp., 17, (2004) 2120.

[14] J. Gottmann, M. Hermans, and J. Ortmann:J. of Las. Micro / Nanoengineering., 8, (2013) 15.

[15] D. Wortmann, J. Gottmann, N. Brandt, and H. Horn-Solle:Opt. Exp., 16, (2008)1517.

[16] Y. Bellouard, A. Champion, B. Lenssen, M. Matteucci, A. Schaap, M. Beresna, C. Corbari, M. Gecevi˘cius, P. Kazansky, O. Chappuis, M. Kral, R. Clavel, F. Bar-rot, J. Breguet, Y. Mabillard, S. Bottinelli, M. Hopper, C. Hoenninger, E. Mottay and J. Lopez:J. of Las. Mi-cro/ Nanoengineering., 7, (2012) 1.

[17] S. Kiyama, S. Matsuo, S. Hashimoto and Y. Morihira: J. Phys. Chem. C, 113, (2009) 11560.

[18] A. Marcinkevi˘cius, S. Juodkazis, M. Watanabe, M. Miwa, S. Matsuo, H. Misawa and J. Nishii: Opt. Lett., 26(5), (2001) 277.

[19] E. Gua, C.W Jeona, H.W. Choia, G. Ricea, M.D. Dawsona, E.K. Illyb and M.R.H. Knowlesb: Proc. of Symposium H on Photonic Processing of Surfaces, Thin Films and Devices, Strasbourg, (2003) p. 462.

[20] Y. Izawa, S. Tanaka, H. Kikuchi, Y. Tsurumi, N. Miyanaga, M. Esashi, M. Fujita: Proc. of 21 IEEE International Conference on Micro Electro Mechanical Systems, Tucson (2008) p. 1084.

[21] D. P. Banks, K. S. Kaur, Ch. Grivas, C. Sones, P. Gangopadhyay, Ch. Ying, J. Mills, S. Mailis, I. Zergioti, R. Fardel, M. Nagel, T. Lippert, X. Xu, S. P. Banks and R. W. Eason: Proc. LAMP2009 - 5th Int. Congress on Laser Advanced Materials Processing, Kobe, (2009) p. 206.

[22] V. Kudriašov, E. Gaižauskas and V. Sirutkaitis: Appl. Phys., 93, (2008) 571.

[23] L. Sudrie, M. Franco, B. Prade and A. Mysyrowicz and P. Corkum: Opt. Commun. 191, (2001) 333.

[24] M. Ams, G.D. Marshall, P. Dekker, M. Dubov, V.K. Mezentsev, I, Bennion and M.J. Withford: IEEE J. Sel. Top. Quantum Electron., 14(5), (2008) 1370.

[25] C. Hnatovsky, R. Taylor, E. Simova, P. Rajeev, D. Rayner, V. Bhardwaj, and P. Corkum: Appl.Phys., A, 84 (1-2), (2006) 47.

[26] S.Ho, M. Haque, P.R. Herman, J. S. Aitchison: Opt.Lett., 37(10), (2012) 1682.

[27] M. Lancry, B. Poumellec, R. Desmarchelier, and B. Bourguignon: Opt. Mat. Expr., 2(12), (2012) 1809.

[28] S. Richter, A. Plech, M. Steinert, M. Heinrich, S. Döring, F. Zimmermann, U. Peschel, E. Bernhard Kley, A. Tunnermann and S. Nolte: Las. Photon. Rev., 6(6), (2012) 787.

[29] Z. Zhi-Yuan, Z. Yi, Z. Wei-Gong, L. Xin, L. Yu-Tong, Z. Jie: Chin. Phys. Lett., 24(2), (2007) 501.

[30] S. Zhu, Y. F. Lu and M. H. Hong: Appl. Phys. Lett., 79, (2001) 1396.

[31] D. Faccio, E. Rubino, A. Lotti, A. Couairon, A. Dubietis, G. Tamošauskas, D. G. Papazoglou and S. Tzortzakis Phys. Rev. A, 85, (2012) 033829.

[32] S. Butkus, E. Gaižauskas, D. Paipulas, Ž. Viburys, D. Kaškelytė, M. Barkauskas, A. Alesenkov and V. Sirutkaitis: Appl. Phys. A, 114(1), (2014) 81.

[33] C. Ohl, M. Arora, R. Dijkink, V. Janve and D. Lohse: Appl. phys. lett. 89, (2006) 074102.

(Received: March 25, 2014, Accepted: July 29, 2014)